LBNL-39296
UC-1240
Preprint

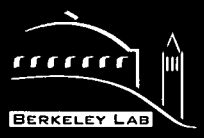

ERNEST ORLANDO LAWRENCE
BERKELEY NATIONAL LABORATORY

Determining Permeability of Tight Rock Samples Using Inverse Modeling

S. Finsterle and P. Persoff
Earth Sciences Division

August 1996
Submitted to
Water Resources Research

DISCLAIMER

LBNL-39296
UC-1240

Determining Permeability of Tight Rock Samples Using Inverse Modeling

Stefan Finsterle and Peter Persoff

Lawrence Berkeley National Laboratory
Earth Sciences Division
University of California
Berkeley, CA 94720

submitted to *Water Resources Research*

August 1996

This work was supported by the Assistant Secretary for Energy Efficiency and Renewable Energy, Geothermal Division, of the U.S. Department of Energy under contract No. DE-AC03-76SF00098.

Determining permeability of tight rock samples using inverse modeling

Stefan Finsterle and Peter Persoff
Earth Sciences Division, Lawrence Berkeley National Laboratory, University of California, Berkeley

Abstract. Data from gas-pressure-pulse-decay experiments have been analyzed by means of numerical simulation in combination with automatic model calibration techniques to determine hydrologic properties of low permeability, low porosity rock samples. Porosity, permeability, and Klinkenberg slip factor have been estimated for a core plug from The Geysers geothermal field, California. The experiments were conducted using a specially designed permeameter with small gas reservoirs. Pressure changes were measured as gas flows from the pressurized upstream reservoir through the sample to the downstream reservoir. A simultaneous inversion of data from three experiments performed on different pressure levels allows for independent estimation of absolute permeability and gas permeability which is pressure-dependent due to enhanced slip flow. With this measurement and analysis technique, we can determine matrix properties with permeabilities as low as 10^{-21} m^2. In this paper we discuss the procedure of parameter estimation by inverse modeling. We will focus on the error analysis which reveals estimation uncertainty and parameter correlations. The impact of systematic errors due to potential leaking and uncertainty in the initial conditions will also be addressed. The case studies clearly illustrate the need for a thorough error analysis of inverse modeling results.

Introduction

The use of standard steady-state methods for the determination of hydrogeologic properties of low permeability rock samples is limited. The main difficulty arises from the need to measure extremely small flow rates with sufficient accuracy. Moreover, the time required to perform the experiment may be prohibitively long. Using fluids of lower viscosity, i.e. gas instead of water, increases flow rates and observable pressure changes within a given time frame. Moreover, gas permeability is in itself of considerable interest in areas such as vapor flow in geothermal reservoirs, pneumatic testing, vadose zone hydrogeology, and contaminant removal by soil vapor extraction.

Methods for determining gas permeability of tight porous media have been proposed by a number of authors (for a review see *Neuzil* [1986]). Transient methods such as the gas-pressure-pulse-decay experiment have been developed [*Brace et al.*, 1968; *Jones*, 1972; *Ruth and Kenny*, 1989] and successfully applied to measure properties of core plugs with a permeability as low as 10^{-21} m^2 [*Ning*, 1993; *Persoff and Hulen*, 1996]. In the gas-pressure-pulse-decay (GPPD) method, gas flows from a quickly pressurized upstream reservoir through the sample to a downstream reservoir. The transient pressure response in both reservoirs is analyzed either analytically or numerically to obtain estimates of permeability and porosity. Analytical solutions have been reviewed and proposed by *Ning* [1993] and *Wu et al.* [1996]. In this study, we use the numerical model TOUGH2 [*Pruess*, 1987, 1991] to simulate the GPPD experiments. The ITOUGH2 code [*Finsterle*, 1993] provides parameter

estimates by automatically matching the calculated to the observed pressure response. As a byproduct of the optimization process, ITOUGH2 performs an extensive sensitivity and error analysis which helps to identify key parameters governing the system behavior, as well as the contribution of individual data points to the solution of the inverse problem. Furthermore, estimation uncertainties and parameter correlations can be examined.

The gas-pressure-pulse-decay measurements available for inverse modeling are summarized in the next section, followed by a discussion of the physical processes, the modeling approach, and inversion techniques used for the numerical analysis of the data. We then discuss the advantage of performing a joint inversion of multiple experiments, and interpret the results based on the error analysis.

Gas pressure pulse measurements

Permeability and porosity was determined on a fine-grained graywacke core plug from the Geysers Coring Project [*Hulen et al.*, 1995]. A schematic of the apparatus used in the experiments, constructed following the design of *Ning* [1993], is shown in Figure 1. Sample plugs, 25 mm in diameter and 50 mm long, were dried at 60 °C, and placed in a sample holder under an oil-controlled confining pressure. The volumes of the upstream and downstream reservoirs were designed to be as small as possible. The total volume of each reservoir, including valves, transducers, and fittings, was determined from gas expansion tests to be 2.08 cm^3. The stainless steel tubing ensures the system compliance to be small. Absolute pressures in the upstream and downstream reservoirs as well as the differential pressure were measured. Temperature was controlled between 26.6 and 26.7 °C.

To conduct a test, the upstream reservoir is rapidly pressurized to a value about 300 kPa above the initial pressure of the system using nitrogen gas. Gas starts to flow through the sample, and the change of pressure with time is observed in both reservoirs. The experiment is repeated on three different pressure levels to isolate the Klinkenberg effect ([*Klinkenberg*, 1941], see discussion below).

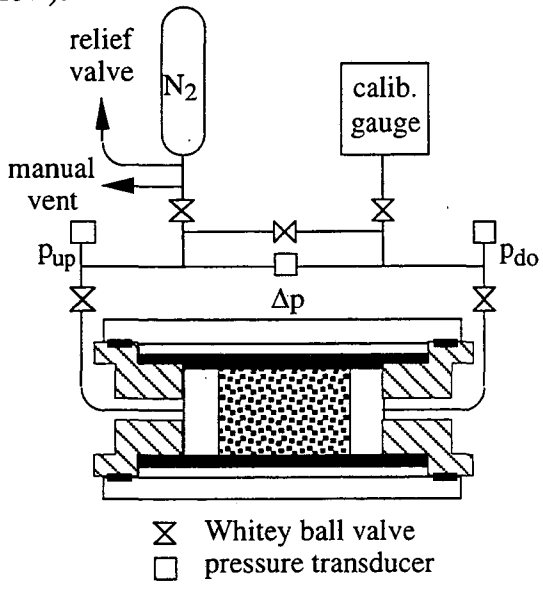

Figure 1. Gas-pressure-pulse-decay apparatus

Physical processes and modeling approach

Modeling of gas flow with Klinkenberg effect

Simulation of the GPPD experiment is performed using the TOUGH2 code [*Pruess*, 1987, 1991]. While TOUGH2 is able to handle non-isothermal flow of multiple components in up to three phases, we discuss here only the terms involved in single-phase gas flow. The integral finite difference method is used to solve the following mass balance equation for an arbitrary subdomain V_n bounded by the surface Γ_n and an inward normal vector $\mathbf{n}$, where q is a local sink and source term:

$$\frac{\mathrm{d}}{\mathrm{d}t}\int_{V_n} M\mathrm{d}V = \int_{\Gamma_n} \mathbf{F}\cdot\mathbf{n}\mathrm{d}\Gamma + \int_{V_n} q\mathrm{d}V \tag{1}$$

The accumulation term M represents mass per unit volume,

$$M = \phi\rho \tag{2}$$

where ϕ is porosity, and ρ is gas density which is a function of pressure and temperature according to the ideal gas law. The mass flux term is given by Darcy's law

$$\mathbf{F} = -k\left(1+\frac{b}{p_{av}}\right)\frac{\rho}{\mu}\nabla p \tag{3}$$

where k is absolute permeability, μ is dynamic viscosity, and p is gas pressure. The term in brackets accounts for enhanced gas slip flow which occurs when the mean free path of the molecules is similar to or larger than the characteristic dimension of the pores. Slip flow is important at low pressures and in small pores, when a significant fraction of molecular collision is with the pore wall rather than with other gas molecules. In (3), b is the Klinkenberg slip factor, and p_{av} is the average pressure. Note that the Klinkenberg slip factor is a characteristic of both the geometry of the pore space and the thermophysical properties of the gas. It is directly proportional to the mean free path λ of the molecules [*Klinkenberg*, 1941]. If performing model predictions with a gas X that is different from the one used in the experiment, for example nitrogen, the Klinkenberg factor has to be rescaled according to the ratios of the respective mean free paths, $b_X : b_{N_2} = \lambda_X : \lambda_{N_2}$. The mean free path can be estimated relying on gas kinetic theory [*Atkins*, 1978]:

$$\lambda = \frac{k_B T}{\sqrt{2}\sigma p_{av}} \tag{4}$$

where k_B is the Boltzmann constant, T is temperature, and σ is the collision cross-section of the gas molecule. Typical collision cross-sections are given by *Atkins* [1978] and reproduced in Table 1, along with the corresponding mean free path at standard conditions and the resulting correction factor for the Klinkenberg parameter, with nitrogen as the reference gas.

Table 1. Collision Cross-sections and Mean Free Path

Gas	σ [10^{-18} m^2]	λ [10^{-6} m]	b_X/b_{N_2}
hydrogen H_2	0.15	0.19	2.06
nitrogen N_2	0.31	0.09	1.00
carbon dioxide CO_2	0.66	0.04	0.47
air	0.30	0.09	1.03
water vapor H_20	0.23	0.12	1.34

Parameter estimation by inverse modeling

The inverse problem, i.e. the determination of parameters from measured data, is solved by minimizing the differences between the observed and simulated system responses, which are assembled in the residual vector **r** with elements

$$r_i = y_i^* - y_i(\mathbf{p}) \tag{5}$$

Here y_i^* is an observation at a given point in space and time, and y_i is the corresponding prediction, which depends on vector **p** of all unknown model parameters, including initial and boundary conditions. If the error structure of the residuals is assumed Gaussian and described by a covariance matrix **C**, the objective function to be minimized is the sum of the squared residuals weighted by the inverse of the prior covariance matrix:

$$Z(\mathbf{p}) = \mathbf{r}^T \mathbf{C}^{-1} \mathbf{r} \tag{6}$$

An iterative procedure is required to minimize the non-quadratic objective function. The Levenberg-Marquardt modification of the Gauss-Newton algorithm [*Levenberg*, 1944; *Marquardt*, 1963] has been found to be the most robust for our purposes. The basic idea of this method is to move in the parameter space along the steepest descent direction far from the minimum, switching continuously to the Gauss-Newton algorithm as the minimum is approached. This is achieved by decreasing a scalar ν, known as the Levenberg parameter, after a successful iteration, but increasing it if an uphill step is taken. The following system of equations is solved for $\Delta\mathbf{p}$ at an iteration labeled k:

$$(\mathbf{J}_k^T \mathbf{C}^{-1} \mathbf{J}_k + \nu_k \mathbf{D}_k)\, \Delta\mathbf{p}_k = -\mathbf{J}_k^T \mathbf{C}^{-1} \mathbf{r}_k \tag{7}$$

Here, **J** is the Jacobian (or sensitivity) matrix with elements $J_{ij} = -\partial r_i/\partial p_j = \partial y_i/\partial p_j$. **D** denotes a matrix of order n (n being the number of parameters to be estimated) with elements equivalent to the diagonal elements of matrix $(\mathbf{J}_k^T \mathbf{C}^{-1} \mathbf{J}_k)$. The improved parameter set is finally calculated:

$$\mathbf{p}_{k+1} = \mathbf{p}_k + \Delta\mathbf{p}_k \tag{8}$$

Under the assumption of normality and linearity, a detailed error analysis of the final residuals and the estimated parameters can be conducted (for details see *Finsterle and Pruess* [1995]). For example, the covariance matrix of the estimated parameter set is given by:

$$\mathbf{C}_{pp} = s_0^2 (\mathbf{J}^T \mathbf{C}^{-1} \mathbf{J})^{-1} \tag{9}$$

where s_0^2 is the estimated error variance

$$s_0^2 = \frac{\mathbf{r}^T \mathbf{C}^{-1} \mathbf{r}}{m - n} \tag{10}$$

with m being the total number of observations.

As a byproduct of calculating the Jacobian matrix $\mathbf{J}$, one can qualitatively examine the contribution of each data point to the solution of the inverse problem as well as the total parameter sensitivity.

The inverse modeling formulation outlined above is implemented in a computer program named ITOUGH2 [*Finsterle*, 1993].

Systematic and random errors

It is very important to appreciate the difference between systematic and random components of the residuals. Provided that the true system behavior were identified, the residuals become equal to the random part of the measurement error. While the individual measurement errors are not known *a priori*, they can be described in statistical terms. This is a key assumption made when deriving the objective function (6) from maximum likelihood considerations. This requires, however, that systematic errors are not existent or have been eliminated. It will be demonstrated in this paper that the impact of systematic errors on the parameter estimates is usually much larger than the one from the noise in the data, even under well-controlled laboratory conditions.

In the following paragraphs we discuss a few potential sources for systematic errors in the analysis of a GPPD experiment. Systematic errors occur in both the data and the numerical simulation. In many cases it is difficult and also irrelevant to distinguish between a systematic modeling error and a systematic error in the data. Systematic errors are simply the result of a conceptual difference between the observation and the corresponding model output. It is more a question of convenience which side of the problem can be better controlled.

The advantage of analyzing laboratory data over field observations is the fact that the geometry as well as initial and boundary conditions are well defined. Nevertheless, a careful design of the testing apparatus is important. For example, the volumes of the upstream and downstream reservoir have to be accurately determined; system compliance effects should be minimized by choosing appropriate equipment materials; leaking has to be avoided by applying sufficient confining pressures; temperature should be kept constant. Deviations from these conditions have to be corrected in the data, if possible, or accurately reproduced in the model. For example, if temperature varies during the course of the experiment, the

pressure data can by adjusted according to the ideal gas law. Alternatively, one could use a non-isothermal model that directly accounts for the temperature dependency of density, viscosity, and Klinkenberg factor. Note that while the latter approach is more difficult to implement, it is also more accurate.

In our study, we use an equation-of-state module that describes the thermophysical properties of air rather than nitrogen. Differences in density and viscosity affect the pressure transient and thus the estimates. Density-viscosity ratios between air and nitrogen differ by a factor of 1.05. This leads to an underestimation of permeability by 5 % if pressure data from an experiment with nitrogen are inversely analyzed using air properties. In this case, the discrepancy between the data and the model output can be compensated after the inversion. In most instances, however, when the model output is affected in a non-linear fashion, such corrections are not possible. The estimation procedure must then be repeated with different assumptions regarding those aspects of the model that are considered uncertain. This may provide some insight into the sensitivity of the results with respect to individual errors. However, the impact of a combination of errors is difficult to assess. In some cases, potential errors can be parameterized and subjected to the estimation process. An example of this approach is discussed later in this paper, where uncertainties regarding initial conditions and potential leaking are addressed.

Analysis of experimental data

We perform a stepwise analysis of the GPPD data to illustrate the process of parameter estimation by inverse modeling. Table 2 summarizes the cases considered in this paper, each of which addresses a specific issue of inverse modeling analysis.

Table 2. Overview of Inverse Modeling Runs

Case	Data	Parameters	Issue
1	pressure level 1	$\log(k)$, $\log(b)$, ϕ	sensitivity analysis, non-uniqueness, parameter correlation
2	pressure level 1, 2, 3	$\log(k)$, $\log(b)$, ϕ	joint inversion, biased estimates due to systematic error
3	pressure level 1, 2, 3	$\log(k)$, $\log(b)$, ϕ, initial pressures, leakage	joint inversion, over-parametrization

In the first case we try to estimate the key parameters of interest, i.e. permeability, Klinkenberg slip factor, and porosity, based on the pressure data from the first experiment which was performed on the lowest pressure level where Klinkenberg effects are expected to be most pronounced. The data and the calculated pressures in the upper and lower reservoir are shown in Figure 2. The dash-dotted line corresponds to the calculated system response with the initial guess for the parameters; the solid line is the match after model calibration. The overall system behavior can be described as follows. The gas pressure in the pore space and the two reservoirs is allowed to reach equilibrium prior to testing. After quick injection of a certain amount of gas into the upstream reservoir, gas starts to flow through the sample

to the downstream volume. Note that the high gas compressibility yields a relatively large storage capacity in the sample itself, leading to a faster pressure decrease in the upstream reservoir and a delayed response in the downstream reservoir. If the experiment were run to steady state, the pressure in the system would be somewhat below the average value of the initial pressure and the applied pressure pulse, the difference being a measure of the amount of gas stored in the core sample.

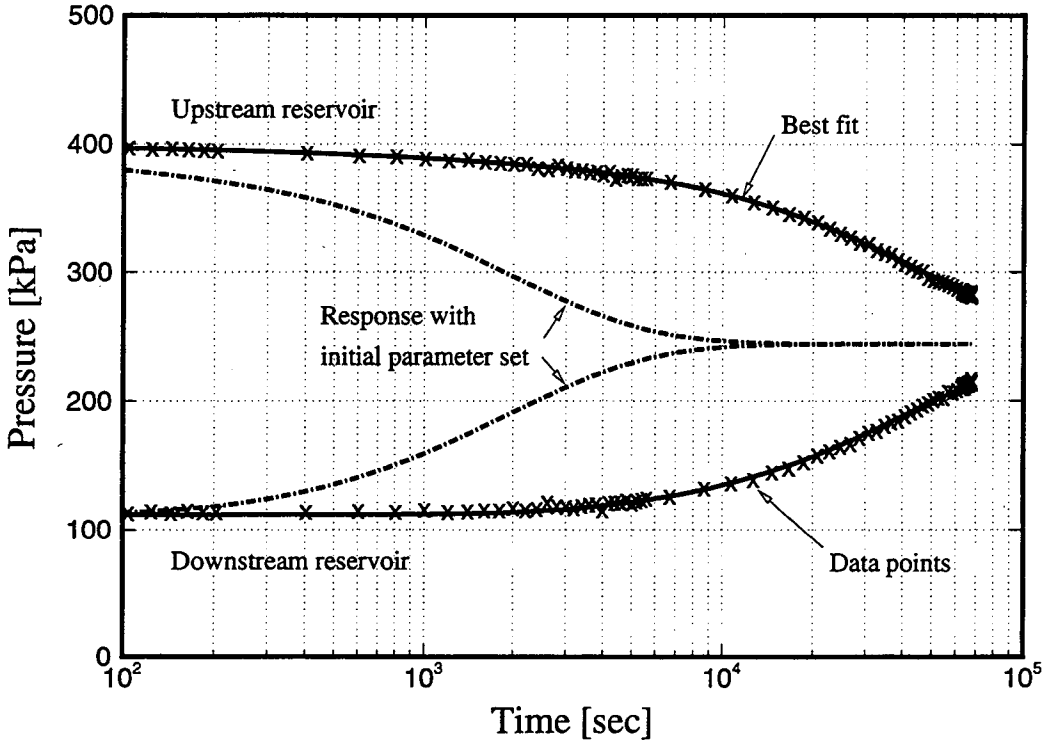

Figure 2. Comparison between measured and calculated pressure transient curves, case 1

It is obvious from Equ. (9) that the sensitivity of the calculated pressure with respect to the parameters of interest is essential for accurate estimation. The elements of the Jacobian matrix **J** provide a means to examine the contribution of each data point to the solution of the inverse problem. In Figure 3, we have plotted the scaled sensitivity coefficients which are defined as the partial derivative of the model output with respect to the input parameters, multiplied by the inverses of the respective prior standard deviations:

$$S_{ij} = \frac{\partial y_i}{\partial p_j} \frac{\sigma_{pj}}{\sigma_{yi}} = J_{ij} \frac{\sigma_{pj}}{\sigma_{yi}} \tag{11}$$

Since only pressure data of equal accuracy are used in this study, an arbitrary value for $\sigma_{yi} = \sigma_y$ of 1000 Pa can be chosen. If data of different types or accuracy are used for the inversion, the prior standard deviations should reflect the expected variance of the final

residuals which is identical to the measurement error if the underlying conceptual model is correct. The choice of σ_{pj} can be based on the variance of an independent parameter measurement, for example if porosity was determined by mercury intrusion porosimetry. In this case, the initial guess is treated as an additional data point, and appropriately weighted in the sense of prior information [*Carrera and Neuman*, 1986]. For this sensitivity analysis, however, it simply scales the sensitivity coefficients, reflecting the expected variation of a parameter.

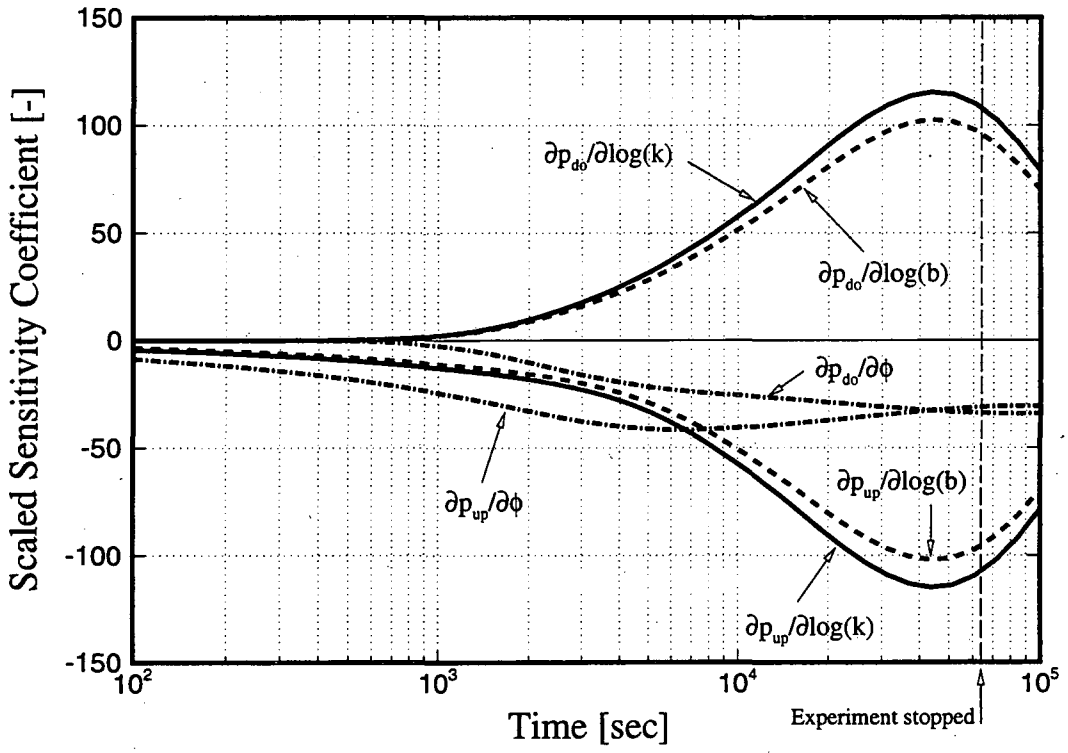

Figure 3. Sensitivity of pressure in upstream and downstream reservoir with respect to permeability, Klinkenberg factor, and porosity as a function of time

The curves in Figure 3 show, for example, that an increase of porosity leads to lower pressures in both reservoirs, whereas an increase in permeability or Klinkenberg factor reduces the upstream pressure, but increases the downstream pressure. This behavior is physically evident. More interesting is the temporal behavior of the sensitivity coefficients. It is obvious that the pressures in the upstream reservoir are immediately affected by changes of the parameters, whereas some time has to pass before the downstream pressure data become sensitive. The absolute sensitivities of $\log(k)$ and $\log(b)$ increase with time and reach a maximum at the inflection point of the pressure transient where gas flow through the sample is sizable and average storativity effects have ceased. The longer the experiment lasts, the less additional information about conductivity can be drawn from the data, since pressure differences and thus flow rates become very small. Eventually the sensitivity coefficients tend to zero. On the other hand, porosity remains sensitive, approaching a constant non-zero

value at late time. As indicated earlier, porosity could be uniquely identified from the steady-state pressure p_∞ and the initial pressure in the upstream and downstream reservoirs of volumes V_{up} and V_{do}, respectively, to be

$$\phi = \frac{(p_{0,up} + p_{0,do})/2 - p_\infty}{p_\infty} \cdot \frac{(V_{up} + V_{do})}{V_{core}} \tag{12}$$

Analysis of the transient data by inverse modeling techniques allows for a reasonably accurate estimation in a much shorter time, taking advantage of the increased sensitivity of the upstream pressure data at early times.

Note that the information provided by the sensitivity plot can be obtained prior to testing, i.e. in the design stage of an experiment. Test duration and most sensitive periods can be identified, or requirements for sensor accuracy can be derived by comparing the results obtained with different standard deviations σ_{yi}. In our case, the experiment was stopped after about 67,500 seconds. This seems to be a good compromise since the incremental information content of the data with respect to permeability and Klinkenberg factor starts to decrease, and sufficient data has been collected to identify porosity.

The inverse modeling results, along with those of the subsequent cases, are summarized in Table 3. From the perfect match and favorable sensitivities one might expect that an accurate estimation of the three parameters is possible. However, an inspection of the covariance matrix of the estimated parameters reveals a relatively large estimation uncertainty. The standard deviation of both permeability and Klinkenberg factor is greater than an order of magnitude. This is a result of a high correlation between the two parameters which yields a non-unique solution. The covariance matrix with the correlation coefficients in the upper triangle is shown in Table 4. The correlation coefficient between $\log(k)$ and $\log(b)$ is very close to -1, i.e. an increase of one parameter can be almost completely compensated by a decrease of the other parameter. This is also reflected in the close similarity of the sensitivity curves shown in Figure 3. The physical explanation is evident from Equ. (3) where k and b become linearly dependent for constant p_{av}. In our simulation, p_{av} varies slightly which makes possible the solution of the inverse problem at hand. A more general measure of parameter dependency is the ratio between the joint and the marginal standard deviation, reported in the last column of Table 3. The standard deviation σ_p is the square root of the diagonal element of matrix $\mathbf{C}_{pp}$ which refers to the joint probability density function, i.e. it takes into account the influence from all correlated parameters. The marginal standard deviation σ_p*, on the other hand, reflects the uncertainty of an estimate provided that all the other parameters are exactly known. Therefore, the ratio σ_p*/σ_p is a measure of how independently a parameter can be estimated. A value close to one signifies an independent estimate, whereas small values indicate a loss of parameter identifiability due to its correlation to other uncertain parameters.

The objective of case 2 is to reduce the statistical correlation between k and b . By statistical correlation we refer to the correlation coefficient reported in Table 4 which is a result of the inverse modeling error analysis. This has to be distinguished from the functional correlation between k and b, such as the one proposed by *Jones* [1972], where a functional form and its coefficients are determined by fitting a curve through presumably independent measurements of k and b. Even though such a correlation may exist mathematically and even physically, the extent to which both parameters can be estimated based on indirect observations depends largely on the type of data and their sensitivity. The correlation

coefficient from the covariance matrix reflects the degree to which the experimental design is able to produce independent estimates.

The pressure dependency of gas slip flow suggests to perform experiments on different pressure levels. A simultaneous inversion of all available data should yield a unique solution. We have analyzed data from three GPPD experiments which were performed using the same core on pressure levels of about 0.3, 1.55, and 2.75 MPa, respectively. The result from the joint inversion is shown in Table 3. First we note the high values for σ_p^*/σ_p which imply that independent estimates have now been achieved. As shown in Table 5, the correlation between $\log(k)$ and $\log(b)$ is weakened from -0.99 in the previous case to -0.52. As expected, this leads to a significant decrease in the estimation error. The estimated values have changed by an order of magnitude compared to the previous analysis, in accordance with the correlation structure discussed above. Comparison of case 1 and case 2 clearly demonstrates that a good match and high parameter sensitivity are not sufficient to guarantee a meaningful solution of the inverse problem. Omitting a detailed analysis of the estimation uncertainty and correlation structure may lead to erroneous interpretation.

Figure 4 shows the agreement between the calculated and observed pressures. While most of the data are reasonably well matched, pressures near the end of the experiments are systematically overpredicted. This is better illustrated in Figure 5 where the residuals are plotted as a function of time. Unlike an ideal residual plot which shows random noise around zero with standard deviation σ_y, Figure 5 reveals a systematic trend in the residuals. The increasing overprediction of pressures with time for the two experiments on the higher pressure level may indicate a leak in the apparatus. Since such a leak is not taken into account in the model, a systematic error is introduced leading to an overestimation of porosity which is increased during the optimization process to compensate for the gas volume leaked to the outside environment.

Table 3. Summary of Inverse Modeling Results: Initial Guess, Best Estimate, Standard Deviation, and Ratio of Marginal and Joint Standard Deviation.

Case	Parameter	Initial guess	Best estimate	σ_p	σ_p^*/σ_p
1	$\log(k$ [m^2])	-19.00	-19.73	1.29	< 0.01
	$\log(b$ [Pa])	7.00	6.32	1.47	< 0.01
	porosity ϕ [%]	1.50	0.96	0.05	0.48
2	$\log(k$ [m^2])	-19.00	-20.67	0.01	0.85
	$\log(b$ [Pa])	7.00	7.30	0.02	0.85
	porosity ϕ [%]	1.50	2.18	0.10	0.99
3	$\log(k$ [m^2])	-19.00	-20.67	0.01	0.78
	$\log(b$ [Pa])	7.00	7.31	0.01	0.80
	porosity ϕ [%]	1.50	1.04	0.04	0.50
	$p_{0,Exp1}$ [bar]	5.00	4.01	0.05	0.69
	$p_{0,Exp2}$ [bar]	17.00	16.88	0.04	0.72
	$p_{0,Exp3}$ [bar]	30.00	29.07	0.04	0.71
	$\log(q_{Exp2}$ [kg/s])	-12.00	-10.79	0.01	0.85
	$\log(q_{Exp3}$ [kg/s])	-12.00	-10.71	0.01	0.86

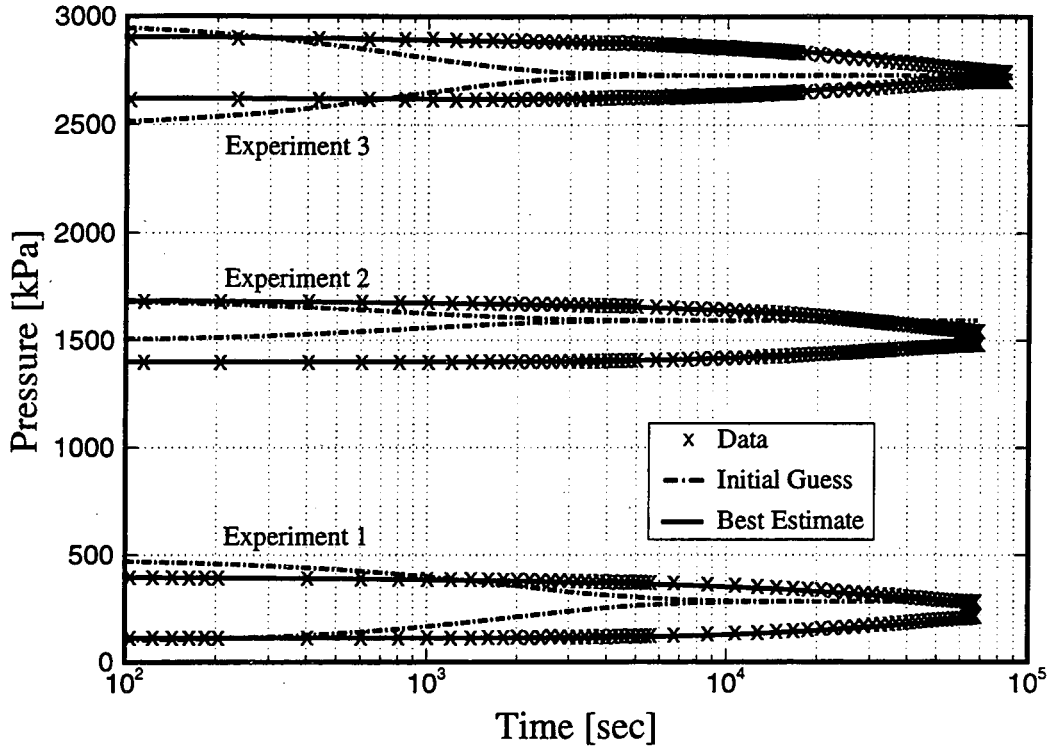

Figure 4. Comparison between measured and calculated pressure transient curves from three simultaneously inverted gas-pressure-pulse-decay experiments, case 2

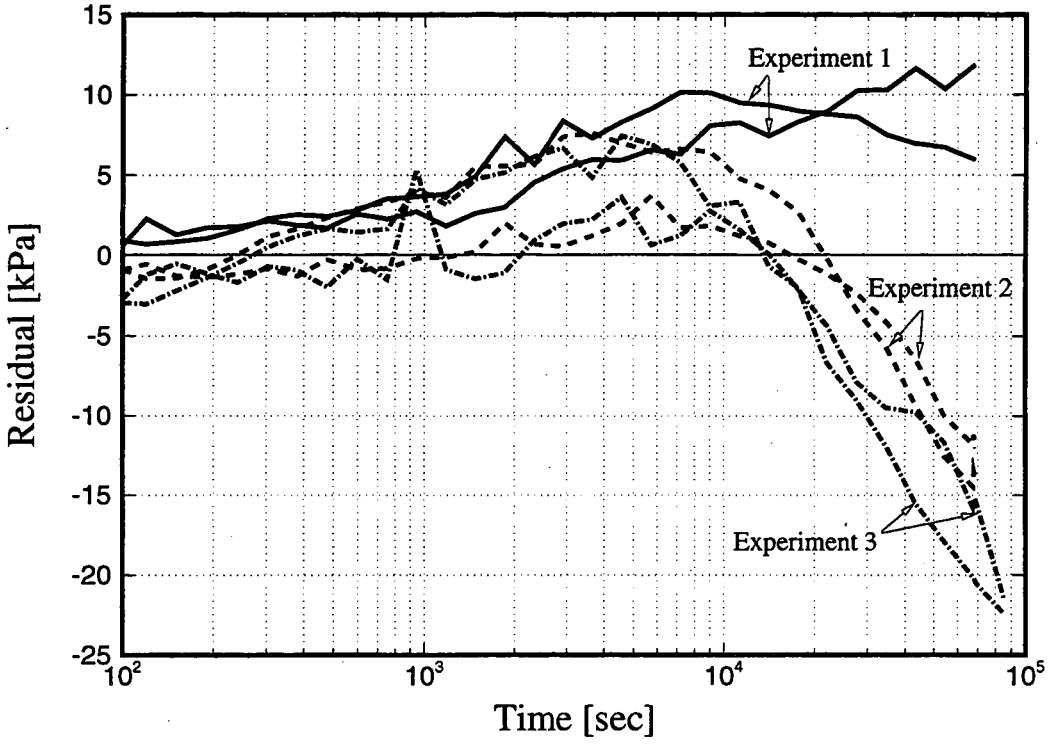

Figure 5. Residuals as a function of time, showing systematic overprediction of pressures at late times, case 2

Table 4. Estimation Covariance Matrix, Case 1

	log(k)	log(b)	porosity
log(k)	1.67	-0.99	-0.87
log(b)	-1.90	2.16	0.87
porosity	-5.79E-4	6.59E-4	2.64E-7

Diagonal contains variances, lower triangle is covariance matrix, and upper triangle is correlation matrix

Table 5. Estimation Covariance Matrix, Case 2

	log(k)	log(b)	porosity
log(k)	1.05E-4	-0.52	-0.12
log(b)	-1.07E-4	4.10E-4	-0.02
porosity	-1.30E-6	-3.62E-7	1.06E-6

Diagonal contains variances, lower triangle is covariance matrix, and upper triangle is correlation matrix

In the final case we try to reduce the impact of systematic errors and discuss the issue of overparameterization. Recall that the estimated parameters strictly refer to the structure of the model used to invert the data. The fact that a systematic error in the conceptual model leads to biased estimates was already seen in the previous case where the porosity estimate seems to be overpredicted due to leakage. In order to account for potential leaking, we introduce a sink term into the model and estimate its flow rate which is assumed to be constant. Using a constant mass flux sink term to model the leak seems appropriate since the transient changes in reservoir pressures are relatively small compared to the pressure drop between the to atmospheric conditions. Furthermore, a test was performed with an impermeable steel plug in the sample holder. Pressure in both the upstream and downstream reservoirs declined exponentially, indicating a constant rate leak to the outside environment.

Besides potential leaks, there is also uncertainty regarding the initial pressure in the upper reservoir. In the previous cases we simply picked the first data point as the initial condition. However, the upstream reservoir undergoes rapid pressurization, causing fluctuations in the data that immediately follow the shut-in of the valves. In order to overcome this problem, we consider the initial pressures in the upstream reservoirs as additional unknown parameters. Accounting for leakage and uncertainty in the initial pressures increases the dimension of parameter vector **p** from 3 to 8. With relatively inaccurate initial guesses for all unknown parameters, ITOUGH2 was able to match the data of all three GPPD experiments very accurately within 6 iterations (Figure 6).

Table 6 summarizes the estimated error variances (Equ. 10) which is a measure of goodness-of-fit. It confirms that the match has been improved by adding the sink term and the initial pressures to the vector of unknown parameters. The standard deviation of the residuals is about 1500 Pa, which is consistent with the fluctuation of the measurement error seen in the residual plot (Figure 7). The best estimates and their uncertainties are again listed in Table 3. While permeability and Klinkenberg factor are not changed between case 2 and case 3, a lower porosity value is realized due to the fact that leakage is explicitly modeled.

The estimated value is consistent with the result from case 1 where less leaking is expected due to the low pressure level of that experiment. The total amount of gas leaked out during experiments 2 and 3 is estimated to be about 0.06 ml and 0.05 ml, respectively.

Parametrization of those aspects of the conceptual model that are most likely to be erroneous is a means to overcome the problem of biased estimation. However, there is a tradeoff between goodness-of-fit and minimum bias on one hand, and estimation uncertainty on the other hand. Increasing the number of parameters always leads to an improvement of the fit, but at the same time increases parameter correlations which results in higher estimation uncertainty. This is seen in case 3 where the standard deviation of porosity is only reduced by a factor of two despite a fourfold improvement of the fit. All ratios σ_p^*/σ_p indicate higher overall parameter correlation. This is most pronounced for porosity, reflecting its correlation to the initial pressure estimates and leakage parameters. Overparameterization of the inverse problem yields higher parameter uncertainties and thus reduces the capabilities of the predictive model.

Carrera and Neuman [1986] introduced a number of model identification criteria which address the issue of overparameterization. We have evaluated Kashyap's criterion to test whether the introduction of five additional parameters into the inverse problem can be justified (for details about the Kashyap criterion the reader is referred to *Kashyap* [1982] and *Carrera* [1984]). The smaller value realized in case 3 (see Table 6) suggests that the improvement of the fit outweighs the increase of estimation uncertainty, thus making case 3 the preferred result of this series of inversions.

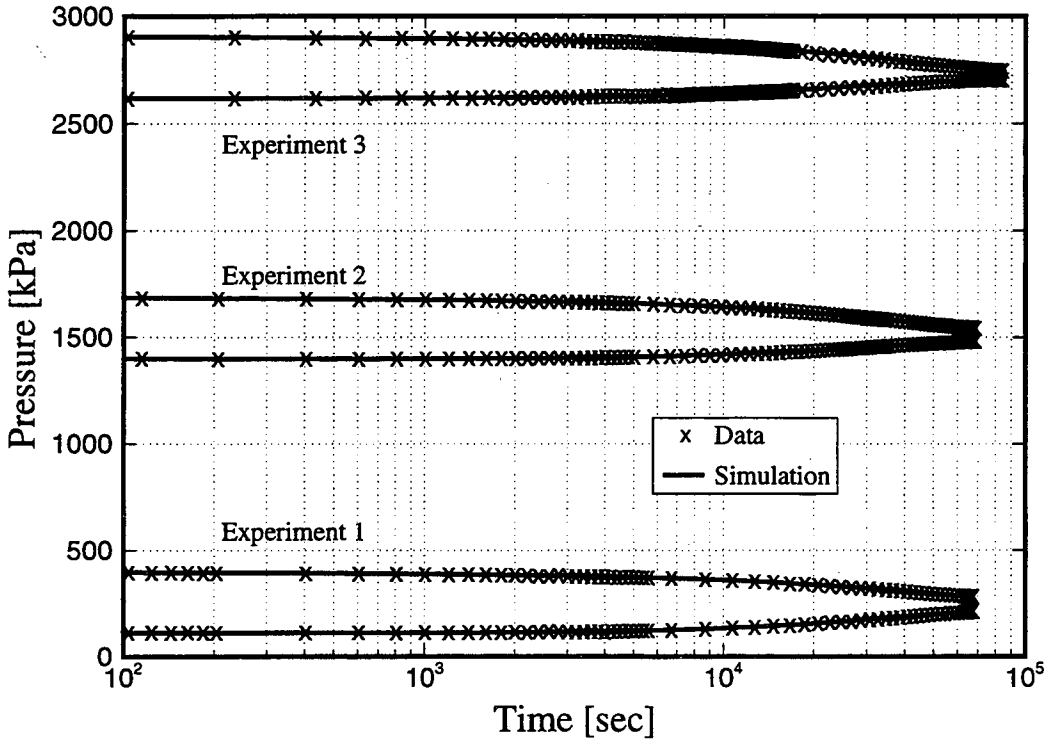

Figure 6. Comparison between measured and calculated pressure transient curves from three simultaneously inverted gas-pressure-pulse-decay experiments, case 3

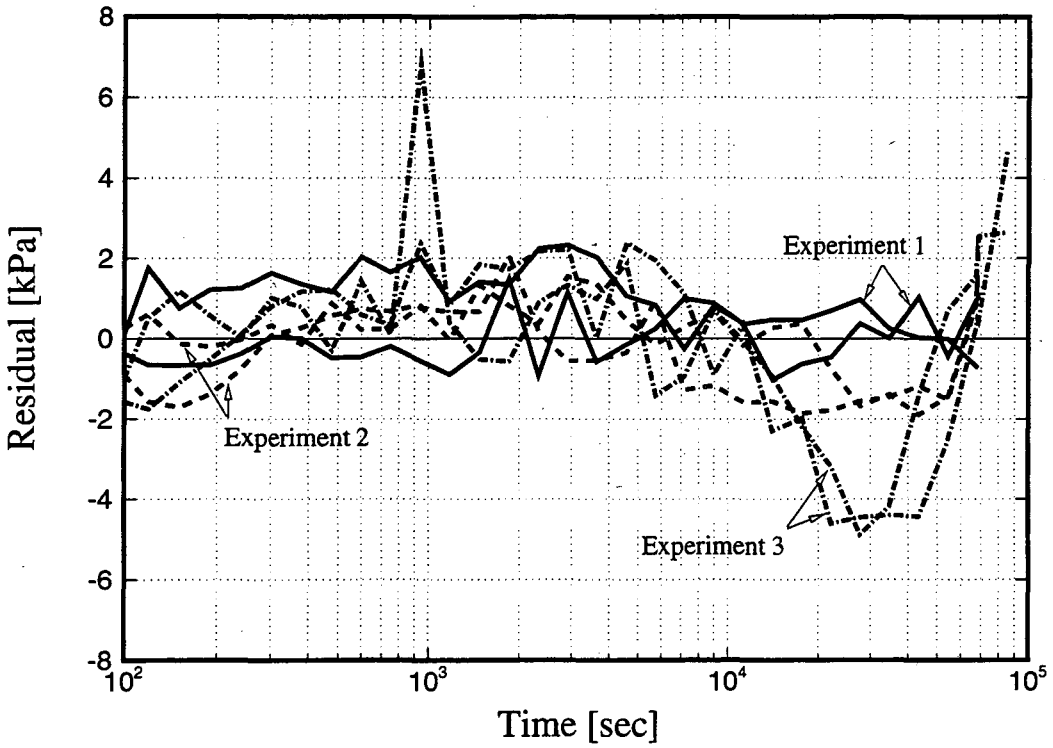

Figure 7. Residuals as a function of time, case 3 (note the different scale from Figure 5)

Table 6. Goodness-of-Fit and Model Identification Criterion

Case	estimated error variance s_0^2	std. dev. of residuals [Pa]	Kashyap criterion
2	48.31	6913.6	12057.1
3	2.44	1533.6	3484.8

Finally we note that the estimates obtained in this study are consistent with the values obtained using an analytical solution [*Persoff and Hulen*, 1995]. Furthermore, the porosity estimate compares reasonably well with values derived for similar cores from Boyles-law gas expansion measurements [*Persoff and Hulen*, 1995]. Permeability and Klinkenberg factor is in good agreement with the correlation model proposed by *Jones* [1972] which was derived for rocks of considerably higher permeability.

Conclusions

Inverse modeling techniques have been used to analyze data from three gas-pressure-pulse decay experiments. Data inversion was performed in three steps with increasing

number of observations and parameters. The main objective of this study was to demonstrate the suitability of GPPD experiments for the determination of hydrogeologic properties, and to discuss the issues of parameter correlation and overparameterization of the inverse problem. The following conclusions can be drawn:

(1) Gas-pressure-pulse-decay experiments are well-suited for determining permeability, Klinkenberg slip factor, and porosity of core samples from very tight formations. The technique is accurate and efficient for core plugs with a permeability as low as 10^{-21} m^2.

(2) The combination of numerical simulation and optimization techniques provides a tool for the estimation of a variety of hydrogeologic properties. The ITOUGH2 code used in this study is capable of handling more complex multiphase flow experiments under both laboratory and field conditions.

(3) Data from different experiments can be analyzed simultaneously using inverse modeling techniques. This improves the basis for the estimation and ensures that consistent parameter values are obtained. In the example discussed in this paper, combining data from different experiments is the key to reducing the correlation between permeability and Klinkenberg slip factor.

(4) A detailed sensitivity analysis provides insight into the information content of individual data points. This information can be used to design and optimize the layout of an experiment (for an example see *Finsterle and Pruess* [1996]).

(5) Achieving a good match between the observed and calculated system response is a necessary, but not sufficient condition for meaningful parameter estimation. Strong correlations among the parameters may lead to high estimation uncertainties or non-unique solutions. Any report of estimated parameter values has to be accompanied by the results of the error analysis.

(6) The ambition to obtain a perfect match often leads to overparameterization of the inverse problem. Error analysis and evaluation of model identification criteria provide some measures to assess whether the chosen parametrization is appropriate.

(7) Systematic errors in either the data or the model lead to a bias in the estimated values which is usually much larger than the statistical estimation uncertainty. Systematic errors should be avoided by careful test design, or by incorporating the related process in a parameterized form into the model.

Acknowledgments. This work was supported by the Assistant Secretary for Energy Efficiency and Renewable Energy, Geothermal Division, of the U.S. Department of Energy under contract No. DE-AC03-76SF00098. Thanks are due to T. Tokunaga, K. Pruess, and T. Sonnenborg for a careful review of the manuscript.

References

Atkins, P. W., Physical chemistry, Freeman & Co., San Francisco, 1978.

Brace, W. F., J. B. Walsh, and W. T. Frangos, Permeability of granite under high pressure, *J. Geophysical Res.*, *73*(6), 2225-2236, 1968.

Carrera, J., Estimation of aquifer parameters under transient and steady-state conditions, Ph.D. Dissertation, Dept. of Hydrology and Water Resour., University of Arizona, Tucson, 1984.

Carrera, J. and S.P. Neuman, Estimation of aquifer parameters under transient and steady state conditions: 1. Maximum likelihood method incorporating prior information, *Water Resour. Res.*, *22*(2), 199-210, 1986.

Finsterle, S., ITOUGH2 User's Guide, Version 2.2, Report No. LBL-35581, Lawrence Berkeley National Laboratory, Berkeley, Calif., August 1993.

Finsterle, S. , and K. Pruess, Solving the Estimation-Identification Problem in Two-Phase Flow Modeling, *Water Resour. Res.*, *31*(4), 913-924, 1995.

Finsterle, S., and K. Pruess, Design and analysis of a welltest for determining two-phase hydraulic properties, in preparation., 1996.

Hulen, J. B., B. A. Koenig, and D. L. Nielson, The Geysers Coring Project, Sonoma County, California - Summary and initial results, Proceedings of World Geothermal Congress, Florence, Italy, 1415-1420, 1995.

Jones, S. C., A rapid accurate unsteady-state Klinkenberg permeameter, *Soc. Petr. Eng. J.*, *12*(5), 383-397, 1972.

Kashyap, R. L., Optimal choice of AR and MA parts in autoregressive moving average models, *IEEE Trans. Pattern Anal. Mach. Intel.*, *PAMI-4*(2), 99-104, 1982.

Klinkenberg, L. J., The permeability of porous media to liquids and gases, *API Drill. and Prod. Prac.*, 200-213, 1941.

Levenberg, K., A method for the solution of certain nonlinear problems in least squares, *Q. Appl. Math.*, *2*, 164-168, 1944.

Marquardt, D. W., An algorithm for least-squares estimation of nonlinear parameters, *J. Soc. Ind. Appl. Math.*, *11*(2), 431-441, 1963.

Neuzil, C. E., Groundwater flow in low permeability environments, *Water Resour. Res.*, *22*, 1163-1195, 1986.

Ning, X., The measurement of matrix and fracture properties in naturally fractured low permeability cores using a pressure pulse method, Ph.D. Thesis, Texas A&M, published as Gas Research Institute Report GRI-93/0103, March 1993.

Persoff, P., and J. B. Hulen, Hydrologic characterization of four cores from the Geysers Coring Project, Proceedings, Twenty-First Workshop on Geothermal Reservoir Engineering, Stanford University, Stanford, California, January 22-24, 1996.

Pruess, K., TOUGH User's Guide, Nuclear Regulatory Commission Report NUREG/CR-4645, NRC, Washington, DC, 1987.

Pruess, K., TOUGH2 - A General-Purpose Numerical Simulator for Multiphase Fluid and Heat Flow, Report No. LBL-29400, Lawrence Berkeley National Laboratory, Berkeley, Calif., May 1991.

Ruth, D. W., and J. Kenny, The unsteady-state gas permeameter, *J. Can. Pet. Tech.*, *28*, 67-72, 1989.

Wu, Y.-S., K. Pruess, and P. Persoff, Steady and transient solutions for gas flow in porous media with Klinkenberg effects, in preparation, 1996.

Ernest Orlando Lawrence Berkeley National Laboratory
One Cyclotron Road | Berkeley, California 94720

Prepared for the U.S. Department of Energy under Contract No. DE-AC03-76SF00098